

Characterization of Concentration-Dependent Infrared Spectral Variations of Urea Aqueous Solutions by Principal Component Analysis and Two-Dimensional Correlation Spectroscopy

Young Mee Jung,^{*,†} Boguslaw Czarnecki-Matuszewicz,[‡] and Seung Bin Kim[†]

Department of Chemistry, Pohang University of Science and Technology,
San 31, Hyojadong, Pohang 790–784, Korea and Faculty of Chemistry,
University of Wrocław, F. Joliot-Curie 14, 50-383 Wrocław, Poland

Received: February 25, 2004; In Final Form: June 14, 2004

The association behavior of urea as a function of urea concentration was elucidated by applying principal component analysis (PCA) and two-dimensional (2D) correlation spectroscopy to concentration-dependent FTIR spectra of aqueous urea solutions. The first principal component revealed changes that occurred during the initial increase in urea concentration, which led to the formation of dimers. The second principal component gave information on changes involving the formation of higher aggregates at higher urea concentration. By applying 2D correlation analysis to two sets of FTIR spectra collected above and below 2 M of urea, which were divided on the basis of the PCA, further details on the association process were extracted. Synchronous and asynchronous 2D correlation spectra constructed from the first group of spectra (urea concentration up to 2 M) identified intensity changes due to the formation of ribbon and chain dimers, while the 2D correlation analysis indicated that for urea concentrations above 2 M, urea undergoes further chain polymerization.

Introduction

The effect of urea on the stability of proteins in aqueous solution is of great interest.^{1–3} Recent studies on the denaturation of proteins by urea have suggested that urea denatures proteins via both direct and indirect (water-mediated) interaction with moieties of different polarity on the protein.⁴ Studies of protein folding in water/urea mixtures have shown that the effectiveness with which urea induces unfolding depends on its concentration. For low concentration, urea molecules tend to stabilize partially folded structures, but at higher concentrations they behave as an effective denaturant.⁵ Despite the widespread use of urea as a denaturing agent, the details of the mechanism of urea–water interaction remains largely unknown.

In the past, two models have been used to describe the properties of aqueous solutions of urea. The first model, known as the Frank–Franks (FF) model,⁶ proposes that the water around a urea molecule is less hydrogen bonded than in bulk water. In this model, the water is regarded as a two-component system of differently ordered molecules of water. The lower degree of ordering of the water molecules around the urea results in an increase in the relative interaction between those water molecules and a protein in solution, which could initiate the unfolding of the protein. Thus, in this approach, urea is treated as a breaker of the water structure. The tendency of urea to weaken the water–water interaction has led it to be called a chaotropic solute under the Hofmeister series nomenclature.⁷ The second model that has been used to describe aqueous solutions of urea argues strongly against the notion that urea acts as a breaker of water structure. This model was initially proposed by Schelman, furthered by Kreschek and Scheraga, and finally extended by Stokes, leading to it being named the

SKSS model.⁸ This model assumes that urea molecules form dimers or oligomers via hydrogen bonds without causing significant changes in the water structure. In support of the SKSS model, molecular simulations^{9,10} have revealed that urea can fit into the water structure as a “waterlike” molecule. More recent studies of impact of urea on water structure by neutron diffraction experiment have shown that urea, because of the large number of sites available for hydrogen bonding, incorporates readily into water, forming hydrogen bonds to water and to itself.¹¹

Given the current lack of knowledge about the properties of aqueous urea solutions, as evidenced by the different assumptions underlying the FF and SKSS models, further investigation into the association properties of urea in water is needed to explain the variation in the denaturing properties of urea solutions with varying urea concentration. The tendency of urea to exhibit appreciable self-association in aqueous solutions was established many years ago by means of molecular dynamics¹² and Monte Carlo¹³ simulation. In addition, on the basis of infrared studies of urea both in crystal and in water solution, Grdadolnik¹⁴ recently showed that urea molecules tend to associate in solution, consistent with the SKSS model. However, to date no detailed analysis of the dependence of the association process on urea concentration has been carried out.

In the present study, we focused on monitoring the association process. We measured infrared spectra of aqueous urea solutions at a wide range of urea concentrations and analyzed the resulting concentration-dependent spectral data using principal component analysis (PCA) and two-dimensional (2D) correlation spectroscopy. The power of these two methods as efficient self-supporting tools for the analysis of processes evolving over some variable (e.g., time, temperature, or concentration) has been demonstrated in two of our previous studies. In one study, we examined the thermal degradation of cellulose by analyzing the OH stretching vibrational region of its infrared spectra,¹⁵ and in the other we elucidated the phase transitions of a Langmuir–

* To whom all correspondence should be sent. Tel: +82-54-279-8121; fax: +82-54-279-3399; e-mail: ymjung@postech.ac.kr.

[†] Pohang University of Science and Technology.

[‡] University of Wrocław.

Blodgett film via its temperature-dependent infrared spectra.¹⁶ In addition, the 2D correlation method has been used to monitor association phenomena in studies of alcohols,¹⁷ with excellent results. In the present work, PCA was used to probe the effects of the process of urea association on the infrared intensities of bands assigned to urea vibrations, while 2D correlation spectroscopy was used to detect the various aggregated species of urea and to establish the urea concentration at which they appear.

Experimental Section

Urea-¹³C was purchased from Sigma Chemical Co. Ltd and used without further purification. For IR measurements, deuterated urea-¹³C was obtained by repeated lyophilization from excess D₂O to completely replace H with D. Deuterated urea-¹³C solutions with different concentrations (0.5–6.0 M) were prepared in phosphate/D₂O buffer at pH 6.6.

IR spectra were measured at 2 cm⁻¹ resolution with a Bomem DA8 FTIR spectrometer equipped with a liquid nitrogen-cooled MCT detector. To ensure a high signal-to-noise ratio, 512 scans were coadded. A flow cell (CaF₂ window, Thermo Spectra-Tech. Inc.) was used in this study.

In the range of IR frequencies measured, D₂O has a very strong band at ~2400 cm⁻¹ because of a stretching vibration, a weak band at ~1550 cm⁻¹ because of a combination of bending and libration vibrations, and a moderate band at ~1210 cm⁻¹ because of a bending vibration.¹⁸ Because the D₂O band at ~1550 cm⁻¹ strongly overlapped with the absorption of bands of urea used in the PCA and 2D correlation analysis, it was necessary to preprocess the IR spectra with an appropriate subtraction procedure. The pretreatment process consisted of the following steps. First, the spectrum of the buffer solution alone was subtracted from the spectra of the urea solutions such that the resulting spectra were more or less featureless in the region between 1300 and 1020 cm⁻¹. The subtracted spectra did not require baseline correction, indicating that the subtraction factors were chosen correctly. Only the range of 1740–1300 cm⁻¹ was used in the PCA and 2D correlation analysis. The pretreatment steps described above were carried out using the GRAMS/386 program (Galactic Inc., Salem, NH).

In the next step, truncated spectra were subjected to denoising procedure based on wavelet transformation (WT). WT denoising works better in recovering the original signal than Savitzky-Golay smoothing and denoising through a Fourier transform.¹⁹ Denoising by WT enables to remove small-amplitude components from experimental peaks without significant shape degradation regardless of their frequencies. This procedure is especially recommended for denoising spectra prior to the 2D correlation analysis where any kind of absorption distortions have drastic impact on the 2D results. It was shown on simulated spectra that in superior manner WT denoising filtered the paraesthetic part from the “truth” part of signal.²⁰ Wavelet filtering was performed using the Wavelet Toolbox by Mathworks. The fifth-level coiflet function was chosen to the denoising process. Selection of threshold method was based on a careful visual inspection of the WT denoised and original spectra. Finally, manual soft thresholding was used. Prior to the PCA calculation, the mean centering operation was applied to the data matrix. PCA was performed using the software Unscrambler (Version 7.01, CAMO, Trondheim, Norway). Synchronous and asynchronous 2D correlation spectra were obtained using the same software as those described previously.¹⁶ In light of recent publications concerning the normalization procedure in 2D correlation analysis,^{21–23} we tested various

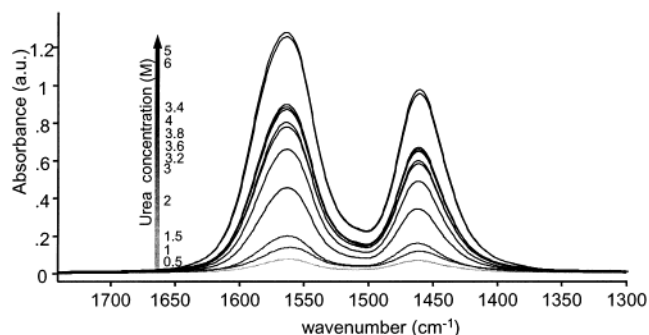


Figure 1. Concentration-dependent FTIR spectra of urea solutions in the region 1740–1300 cm⁻¹ after the final pretreatment process.

TABLE 1: Values of the Positions, Absorbance Maxima, and the Absorbance Ratios for the $\nu(\text{CO})$ and $\nu_{\text{as}}(\text{CN})$ Bands for Analyzed Urea Solutions

urea concentration (M)	$\nu(\text{CO})$ (cm ⁻¹)	$\nu_{\text{as}}(\text{CN})$ (cm ⁻¹)	Abs _{max} $\nu(\text{CO})$	Abs _{max} $\nu_{\text{as}}(\text{CN})$	absorbance ratio (Abs _{C=O} /Abs _{CN})
0.5	1562	1462	0.0760	0.0699	1.09
1.0	1562	1462	0.1325	0.1131	1.17
1.5	1563	1462	0.1991	0.1598	1.25
2.0	1563	1462	0.4563	0.3445	1.32
3.0	1563	1461	0.6593	0.4904	1.34
3.2	1563	1461	0.7723	0.5778	1.34
3.4	1564	1461	0.8994	0.6727	1.34
3.6	1564	1461	0.8023	0.5986	1.34
3.8	1564	1461	0.8717	0.6507	1.34
4.0	1564	1461	0.8836	0.6596	1.34
5.0	1564	1460	1.2748	0.9744	1.31
6.0	1564	1460	1.2549	0.9534	1.32

methods. We found that the best results were obtained using non-normalized data.

Results and Discussion

Concentration-Dependent FTIR Spectra. Figure 1 shows the concentration-dependent spectra of urea solutions in the region 1740–1300 cm⁻¹. The assignments of the bands in this region were made on the basis of data from a previous study.²⁴ That study presented a detailed vibrational analysis of the gas-phase spectra of the ¹³CO(ND₂)₂ isotopomer, made on the basis of the calculated potential energy distribution (PED).²⁴ Both experimental and calculation results have pointed to the presence of two bands in the region 1740–1300 cm⁻¹. One calculated band at 1558 cm⁻¹ was assigned to the CO stretching vibration and, according to the calculated PED, has ca. 60% $\nu(\text{CO})$ character. The other band at 1469 cm⁻¹ was assigned to the antisymmetrical CN stretching vibration on account of the ca. 73% contribution from the $\nu_{\text{as}}(\text{CN})$ vibration. In agreement with these previous results,²⁴ the spectra in Figure 1 clearly show bands at around 1560 and 1460 cm⁻¹, which we assign to the $\nu(\text{CO})$ and $\nu_{\text{as}}(\text{CN})$ vibrations, respectively. The results of a simple analysis of the band positions and absorption maxima are collected in Table 1.

Figure 2 shows plots of the concentration-dependent FTIR spectral data given in Table 1. As the urea concentration increases, the $\nu(\text{CO})$ and $\nu_{\text{as}}(\text{CN})$ bands have small but distinct 2 cm⁻¹ shift into a higher and a lower frequency, respectively (Figure 2a). This shift likely indicates the urea concentration at which the degree of urea self-association becomes appreciable, leading to shifts of the bands because the strengths of the urea–water and urea–urea complexes are different.¹² In addition, the concentration dependencies of the absorbance maxima (Figure 2b) for the two bands are very irregular, mainly for concentra-

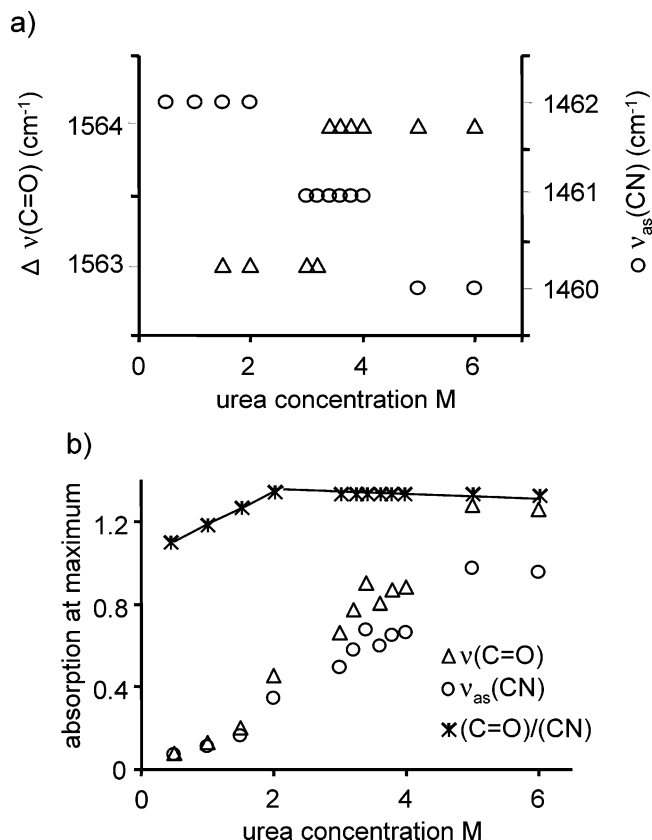
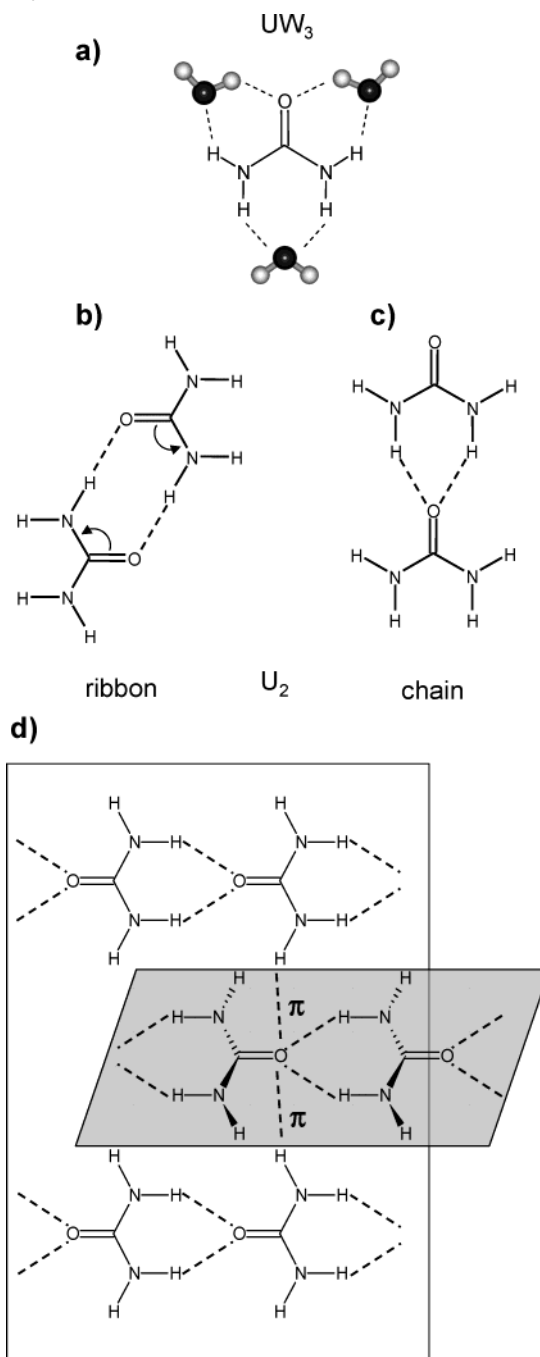


Figure 2. Positions (a) and absorbance values (b) at the absorption maxima of the $\nu(\text{C}=\text{O})$ (Δ) and $\nu_{\text{as}}(\text{CN})$ (\circ) bands. The plot (*) represents the absorbance ratios for the two bands ($\text{Abs}_{\text{C}=\text{O}}/\text{Abs}_{\text{CN}}$) versus concentration of urea solution.

tions higher than 2 M. Any changes in the intermolecular arrangement of the urea molecules in solution should affect the polarities of their $\text{C}=\text{O}$ and $\text{C}-\text{N}$ bonds. Therefore, the observed nonlinear variations of the absorbance values with increasing urea concentration seem to point on developing of the association process of urea that apparently is connected with the intermolecular rearrangement. In the absence of any association, the ratio of the intensities of the absorptions due to the $\nu(\text{CO})$ and $\nu_{\text{as}}(\text{CN})$ vibrations should be insensitive to the urea concentration. However, as shown in Figure 2b, this ratio changes with increasing urea concentration. Therefore, the previous claim based on analyses of the $\nu(\text{CN})$ vibration in Raman spectra of aqueous solutions of urea,²⁵ that intermolecular urea–urea hydrogen bonds do not exist in such solutions, is inconsistent with the present data.

To interpret the changes in the absorbance of the $\nu(\text{CO})$ and $\nu_{\text{as}}(\text{CN})$ bands with increasing urea concentration, it is important to realize that different kinds of urea aggregates could potentially form in this system. Scheme 1 presents more representative urea–water and urea–urea configurations revealed by both theoretical and experimental studies concerning a gas and condense phase. Using density functional theory (DFT), Lee et al.²⁶ found that the structure UW_3 (Scheme 1a) is the most energetically favorable urea–water configuration. Two urea molecules not bridged by water molecules could appear as a ribbon (linear) and chain (cyclic) dimer U_2 (Scheme 1b and 1c, respectively). Theoretical studies of urea coplanar dimers^{26–28} indicate that in a gas phase due to the resonance-assisted hydrogen-bonding effect²⁹ the ribbon dimer is more stable than the chain dimer. The problem whether at higher urea concentration the molecules associate exclusively as dimers or also form larger scale clusters was analyzed by means of molecular

SCHEME 1: Structures of Urea in a Complex with Water (a), Ribbon Dimer (b), Chain Dimer (c), and in the Crystalline State (d)



dynamics (MD) simulations.^{30–32} It was shown that as the oligomer grows, in contrast to more stable ribbon structure developed for dimer, association into the chain structure is progressively stabilized.

Crystallographic data³³ show that in crystalline urea the molecules line up as infinite chains such that the planes of the molecules in adjacent chains are orthogonal (see Scheme 1d). Moreover, studies on modeling the crystal structure of urea by ab initio calculations³⁴ and MD simulation³⁰ reveal a large heterogeneity in the interactions between the urea molecules in the orthogonal chains. In light of the above presented facts, one can expect that IR spectrum of urea in a range of $\nu(\text{CO})$ and $\nu_{\text{as}}(\text{CN})$ vibrations is a result of many, strongly overlapped bands attributed to the different types of urea structure. We therefore conclude that a detailed and careful analysis of the absorbance

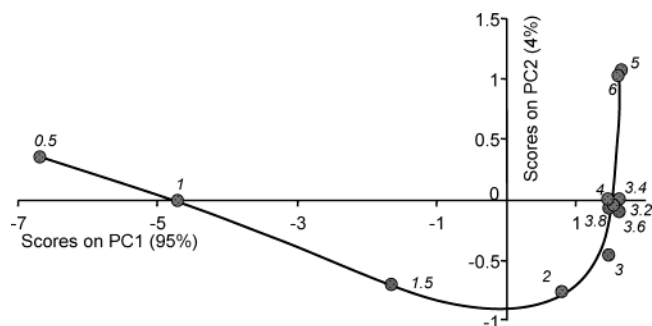


Figure 3. Scores on first two PCs for the concentration-dependent FTIR spectra of urea solutions.

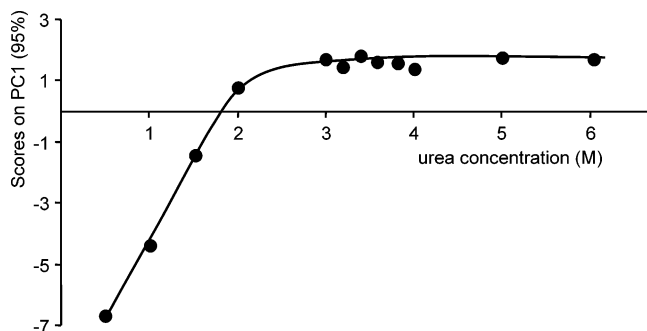


Figure 4. Scores on the first PC versus urea concentration for the FTIR spectra of urea solutions.

changes of the two almost symmetrical bands reported in Figure 1 should yield information on the process of urea aggregation.

To obtain a more detailed picture of the spectral changes as a function of urea concentration, we employed two advanced methods of spectral analysis. First, the spectra were subjected to PC analysis and then were processed by 2D correlation spectroscopy.

PCA of Concentration-Dependent FTIR Spectra. Figure 3 shows a PCA score plot based on the concentration-dependent FTIR spectra shown in Figure 1. The spectra of solutions containing 0.5–1.5 M urea have negative principal component 1 (PC1) scores spread out over six units, whereas the 2–6 M urea spectra have positive PC1 scores and form a tight cluster. Most probably, the first PC that from definition relates to some physical phenomenon that induces a greatest amount of variations in the data here reflects the association process of the urea molecules. Therefore, given that PC1 explains 95% of the spectral variation, it seems that the association process controls most of the spectral variations in the 1740–1300 cm^{-1} region as a function of urea concentration. To analyze this in greater detail, Figure 4 shows the variation in PC1 scores as a function of urea concentration. The trend in the PC1 scores with increasing urea concentration shows a clear change between 2 and 3 M urea, indicating a change in the interactions in the system. Judged by literature data,^{11,30} most probably above the 3 M concentration clusters of different size are formed. However, from the PC1 scores the size of the clusters cannot be guessed.

Further details on this system can be obtained by considering the principal component 2 (PC2) scores in Figure 3, because the group of spectra with positive PC1 scores is separated along the PC2 axis. The lowest PC2 score is observed for the 2 M urea spectrum, and the PC2 scores then progressively increase with increasing urea concentration. Thus, the observation that the PC2 scores vary as the urea concentration is increased from 2 to 6 M indicates that the association process is not limited to a single type of urea associate but involves the formation of

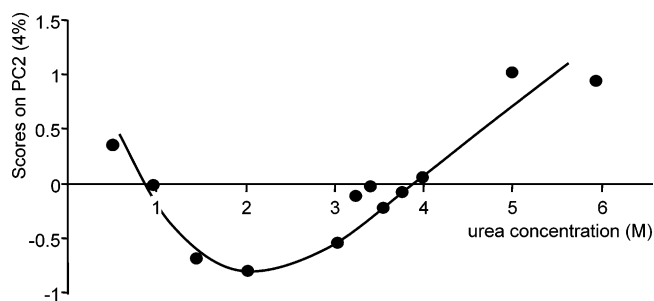


Figure 5. Scores on the second PC versus urea concentration for the FTIR spectra of urea solutions.

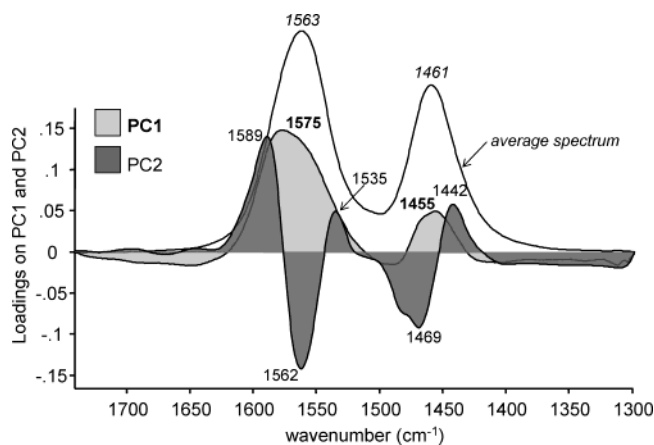


Figure 6. Loadings for first two PCs for the concentration-dependent FTIR spectra of urea solutions combined with an averaged spectrum obtained by averaging the spectra of all urea solutions.

different urea associates. This trend is very clear in Figure 5, which shows the variation in the PC2 scores as a function of urea concentration. However, given that PC2 accounts for only 4% of the total intensity changes, we conclude that the major intensity changes occur during the initial stages of association, with the further association having only a minor effect on the intensities of the two bands, $\nu(\text{CO})$ and $\nu_{\text{as}}(\text{CN})$.

The PC1 and PC2 loadings plots are presented in Figure 6. High positive PC1 loadings distributed over the broad ranges of 1610–1520 cm^{-1} and 1480–1420 cm^{-1} are strongly related with the association process starting for concentration above 2 M. Both the position and shape of the PC1 loadings peaks are very similar to these in original spectra presented in Figure 6 by the averaged spectrum of the concentration-dependent FTIR spectra of urea. With respect to the averaged spectrum, the PC1 loading peak at 1575 cm^{-1} is shifted to higher wavenumbers by 8 cm^{-1} , while the PC1 loading peak at 1455 cm^{-1} is shifted to lower wavenumbers by 6 cm^{-1} . The asymmetrical shape of these two PC1 loadings peaks indicates that probably there is more clusters than only one size. As it can be expected, the energies of the $\nu(\text{CO})$ and $\nu_{\text{as}}(\text{CN})$ vibrations in the different urea clusters that are likely to form do not differ considerably. As a consequence, well-resolved single peaks corresponding to individual urea species are not observed; instead, we find only two broad and structured peaks in the range of the $\nu(\text{CO})$ and $\nu_{\text{as}}(\text{CN})$ vibrations, respectively. More deeply, their structure can be monitored by PC2 loadings.

In the range of the $\nu(\text{CO})$ vibration, the PC2 loadings plot has two positive peaks, at 1589 and 1535 cm^{-1} , and one negative peak at 1562 cm^{-1} . The peak at 1589 cm^{-1} is related to the spectra for the two highest concentrations (5 and 6 M). The peak at 1535 cm^{-1} is related to the spectra for all concentrations above 3 M, while the negative peak at 1562 cm^{-1} is related to

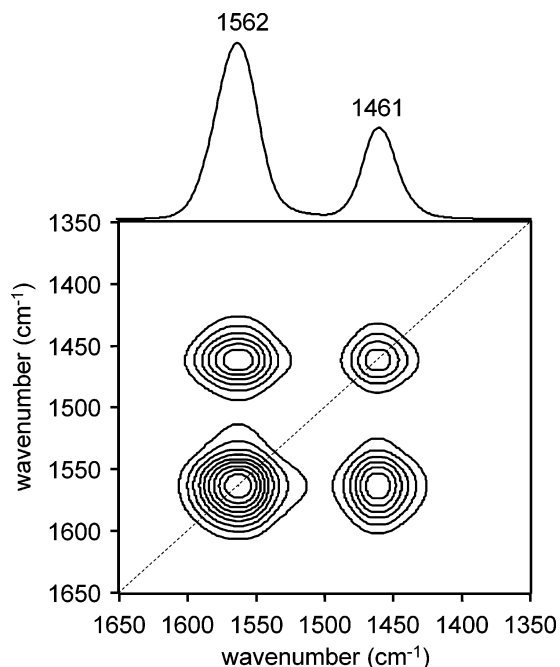


Figure 7. Synchronous 2D IR correlation spectrum with a power spectrum along the diagonal line (top) in the synchronous spectrum constructed from the first set (0.5–2 M) of concentration-dependent spectral changes.

the spectra of the 2 and 3 M urea solutions. In the range of the $\nu_{\text{as}}(\text{CN})$ vibration, the PC2 loadings plot is composed of one negative asymmetric peak at 1469 cm^{-1} with a shoulder and one positive symmetric peak at 1442 cm^{-1} . The first of these peaks is related to the spectra for the concentration range 1.5–3 M, and the second is related to the spectra for the two highest concentrations.

2D Infrared Correlation Analysis. The final assignments of all these peaks are facilitated by employing 2D correlation spectroscopy. The benefits of such complementary studies have been previously demonstrated in the analysis of infrared spectra of complicated biological systems.^{15,34} The PCA results presented above indicate that the measured spectra fall into two groups, one comprising spectra of dilute solutions (0.5–2 M urea), and the second comprising spectra of solutions with higher urea concentrations (3–6 M). Guided by this finding, 2D correlation spectra were calculated for these two sets of spectra. Figure 7 presents the synchronous 2D correlation spectrum and a power spectrum generated from the first set of concentration-dependent spectra (0.5–2 M). In the synchronous 2D correlation spectrum, the two prominent peaks at 1562 and 1461 cm^{-1} are strongly positively correlated. Moreover, the power spectrum shows that the intensity variations caused by increasing the urea concentration induce an unequal change in the absorptions of the two bands, with a larger intensity variation occurring on the side of the $\nu(\text{CO})$ band compared to the $\nu_{\text{as}}(\text{CN})$ band. Primary source of this disproportion is the resonance-assisted effect that leads to an increase of the polarity of the $\text{C}=\text{O}$ bond but a decrease of the polarity of the $\text{C}-\text{N}$ bond during the association process, mainly at the stage of dimer formation.

The corresponding asynchronous spectrum and a slice spectrum at 1585 cm^{-1} are shown in Figure 8. Such asynchronous spectrum analyzed through appropriate slices enhances the resolution of individual overlapping components. From the slice spectrum at 1585 cm^{-1} , it is possible to discriminate additional peaks at 1562 and 1469 cm^{-1} in the range of the absorption of the $\nu(\text{CO})$ and $\nu_{\text{as}}(\text{CN})$ bands, respectively, which unambigu-

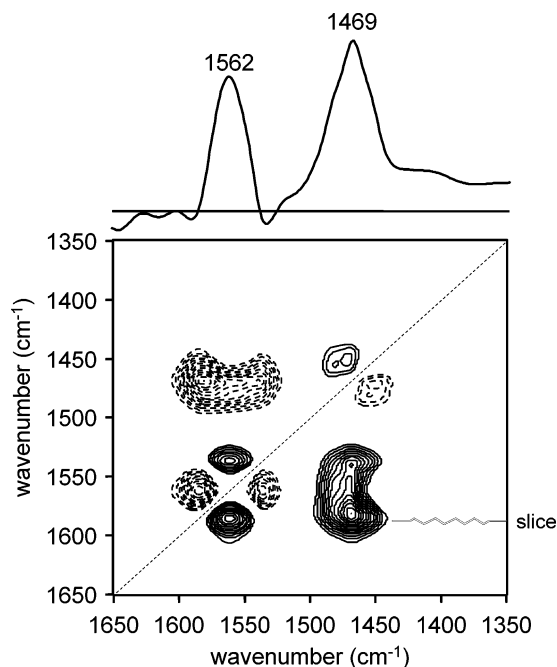


Figure 8. Asynchronous 2D IR correlation spectrum with a slice spectrum (top) extracted along 1585 cm^{-1} in the asynchronous spectrum constructed from the first set (0.5–2 M) of concentration-dependent spectral changes. Solid and dashed lines represent positive and negative cross-peaks, respectively.

ously shows that the urea solutions with concentrations of 0.5–2 M contain different kinds of urea aggregates. The positions of the peaks in the slice spectrum are in very good agreement with those detected by PC2. Table 2 lists the frequencies of the peaks detected by both PCA and 2D correlation analysis. Consideration of both the PCA and 2D correlation analysis results facilitates the assignment of the peaks detected in each procedure.

In the $\nu(\text{CO})$ vibration region of the spectra from 0.5 to 2.0 M urea solutions, the two exploratory methods showed three peaks. The absorption maxima of these peaks are around 1585, 1562, and 1537 cm^{-1} . The peaks at 1562 and 1537 cm^{-1} are assigned to the chain and ribbon dimers respectively,³² and the peak at 1585 cm^{-1} can be assigned to monomeric urea or terminal $\text{C}=\text{O}$ groups of chain dimers that are not directly involved in urea–urea hydrogen bonding.

In the $\nu_{\text{as}}(\text{CN})$ vibration region, a single peak is observed at $\sim 1469\text{ cm}^{-1}$, which is assigned to the ribbon dimer. This peak lies above the maximum of the $\nu_{\text{as}}(\text{CN})$ band, which had an average value of 1461 cm^{-1} , providing clear evidence of the influence of the resonance-assisted effect on the strength of the $\text{C}-\text{N}$ bond. It can be supposed that the frequency couples at $(1562, 1461)\text{ cm}^{-1}$ and $(1537, 1469)\text{ cm}^{-1}$ are signatures of the chain and ribbon structures, respectively. The peak at $(1585, 1450)\text{ cm}^{-1}$ originates from groups that are not engaged in urea–urea hydrogen bonding. However, because the urea–water hydrogen bonds are weaker than those between urea molecules, this peak can be attributed to urea molecules involved in urea–water hydrogen bonds. The asynchronous peaks strongly support the above assignments. First, a strong asynchronicity at $(1585, 1469)\text{ cm}^{-1}$ is developed between intensities arising from vibrations assigned to bonds that are not involved in association and those involved in dimeric forms. Second, a much weaker asynchronicity is developed between bands attributed to ribbon and chain structures.

Figures 9 and 10 show the synchronous 2D correlation spectrum with a power spectrum and the asynchronous 2D

TABLE 2: Positions of Peaks (cm^{-1}) Detected by Means of PCA and 2DCOS Procedures in the Region of the $\nu(\text{CO})$ and $\nu_{\text{as}}(\text{CN})$ Vibrations

PCA		2DCOS, set (0.5–2 M)			2DCOS, set (3–6 M)		
PC1	PC2	synchronous	asynchronous	assignments	synchronous	asynchronous	assignments
1575	1589	1562	1585	$\nu(\text{CO})$ in monomer or terminal C=O of chain dimer	1564	1570	$\nu(\text{CO})$ in terminal C=O of oligomer
		1562	1562	$\nu(\text{CO})$ HB ^a in chain dimer		1545	$\nu(\text{CO})$ in oligomer
		1535	1537	$\nu(\text{CO})$ HB ^a in ribbon dimer			
1455	1469	1461	1469	$\nu_{\text{as}}(\text{CN})$ in ribbon dimer	1458	1474	$\nu_{\text{as}}(\text{CN})$ in terminal of oligomer
	1442		1450	$\nu_{\text{as}}(\text{CN})$ in monomer		1446	$\nu_{\text{as}}(\text{CN})$ in oligomer

^a HB: CO group involved in hydrogen bonding.

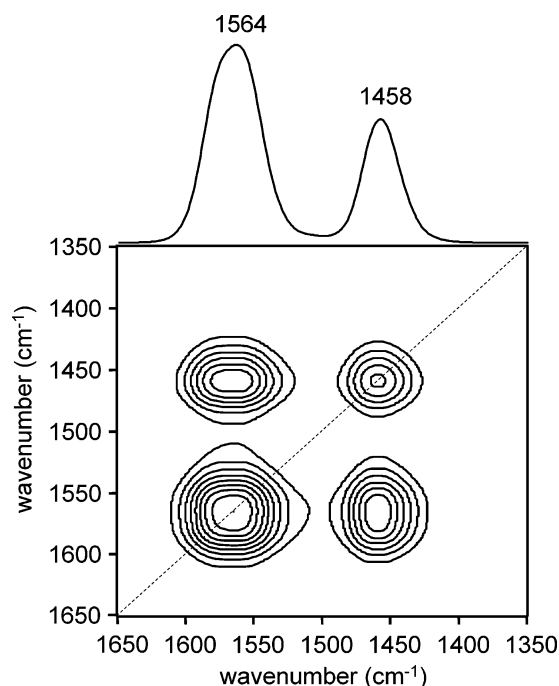


Figure 9. Synchronous 2D IR correlation spectrum with a power spectrum along the diagonal line (top) in the synchronous spectrum constructed from the second set (3–6 M) of concentration-dependent spectral changes.

correlation spectrum with a slice spectrum at 1545 cm^{-1} generated from the second set of spectra (3–6 M urea), respectively. As was observed in the raw spectra, the peaks in the power spectrum correlated with the $\nu(\text{CO})$ and $\nu_{\text{as}}(\text{CN})$ vibrations are shifted to higher and lower frequency, respectively, with increasing urea concentration. Because the peaks are formed by the overlapping of bands with different extinction coefficients assigned to different urea aggregates, it is not possible to analyze the association process in detail only on the basis of the peak positions. In fact, any analysis aimed at elucidating the inter- or intramolecular interactions from infrared or Raman bands must go beyond simply inspecting the band positions. One feature that can be seen is that, in this concentration range, the $\nu(\text{CO})$ band exhibits larger intensity variations than the $\nu_{\text{as}}(\text{CN})$ band. Given that the change in infrared intensity is correlated with the change in bond polarity, our data suggest that, mainly around 2 M urea, the association process induces greater changes in the polarity of the C=O bonds than the C–N bonds.

The frequencies of the peaks detected in the synchronous (Figure 9) and asynchronous (Figure 10) 2D correlation spectra are also given in Table 2. On the basis of the literature facts mentioned earlier, one can postulate that for urea concentrations higher than 3 M linear chain oligomers developed in the system. Such associates contain two environments for the C=O

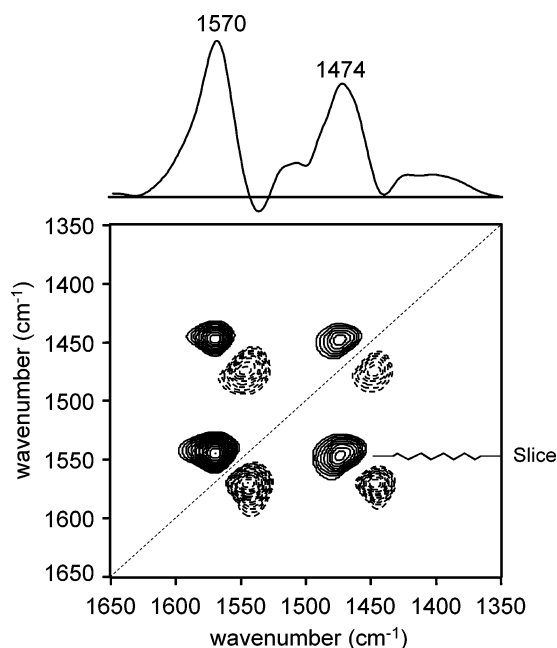


Figure 10. Asynchronous 2D IR correlation spectrum with a slice spectrum (top) extracted along 1545 cm^{-1} in the asynchronous spectrum constructed from the second set (3–6 M) of concentration-dependent spectral changes. Solid and dashed lines represent positive and negative cross-peaks, respectively.

groups: at the ends and inside of the chains. Moreover, at higher urea concentrations (5–6 M), complexes in which the oxygen atom participates in more than two hydrogen bonds should be considered. Hence, the manifold system is characterized by the following frequency couples in the C=O and the CN vibration regions: $1570, 1545\text{ cm}^{-1}$, and $1474, 1446\text{ cm}^{-1}$. The bands in the frequency couple $(1570, 1446)\text{ cm}^{-1}$ exhibit strong asynchronicity, supporting the assignment of these bands to vibrations that are relatively unaffected by the association process (i.e., C=O and C–N terminal fragments that are not directly engaged in the hydrogen bonds of the oligomers). The second peak at $(1545, 1474)\text{ cm}^{-1}$ is clearly resolved in the asynchronous spectrum and can be assigned to vibrations of groups participating in the association process. Even the simple fact that the asynchronous plots for the two different ranges of urea concentration (Figures 8 and 10) have dissimilar patterns reveals that urea association goes through different types of oligomers depending on a concentration of urea.

The present results suggest the following pattern of urea association with increasing urea concentration. At low urea concentration, single urea molecules form complexes with water. On increasing urea concentration, ribbon and chain dimers develop, with the concentration of dimeric urea reaching a maximum around urea concentration of 2 M. Further increase of urea concentration leads to the formation of oligomeric chains of urea molecules.

Conclusions

Urea association in aqueous urea solutions has been studied through the analysis of infrared spectra by means of PCA and 2D correlation spectroscopy. In the PCA, the spectral changes with increasing urea concentration could be reconstructed using two principal components. The first principal component revealed changes that occurred during the initial increases in urea concentration, which led to the formation of urea dimers, and the second principal component unmasked the formation of higher aggregates at higher urea concentrations. The dimerization process reached maximum efficiency at urea concentration of 2 M. The changes in the bands corresponding to the $\nu(\text{CO})$ and $\nu_{\text{as}}(\text{CN})$ vibrations induced by the dimerization process were much stronger than those induced by association into higher oligomers at higher urea concentration. On the basis of the PCA results, the solutions were divided into two groups (0.5–2 M and 3–6 M). By applying 2D correlation analysis to the raw spectra of each of these groups, further details on the association process were extracted. For spectra from solutions with urea concentrations of less than 3 M, intensity changes due to the formation of ribbon and chain dimers were identified. For the solutions with higher urea concentrations, the distribution of spectral changes detected by 2D correlation spectroscopy indicated that, when the urea concentration is increased to above 2 M, further association into higher order structures occurs. Our finding that the association process of urea in solution has the two distinct stages indicates that a molecular description of how urea interacts with a protein should be correlated with the association profile. This should be also taken into account in a discussion on the effect of urea on protein structure if systems of different concentration of urea solutions are considered.

Acknowledgment. This work was supported by the Korea Research Foundation (2003-015-C00272).

References and Notes

- (1) Scholtz, J. M.; Barrick, D.; York, E. J.; Stewart, J. M.; Baldwin, R. L. *Proc. Natl. Acad. Sci. U.S.A.* **1995**, *92*, 185.
- (2) Zou, Q.; Habermann-Rottinghaus, S. M.; Murphy, K. P. *Proteins: Struct., Funct., Genet.* **1998**, *31*, 107.
- (3) Caflisch A.; Karplus, M. *Structure* **1999**, *7*, 477.

- (4) Bennion B. J.; Daggett, V. *Proc. Natl. Acad. Sci. U.S.A.* **2003**, *100*, 5142.
- (5) Johnson, C. M.; Fresht, A. R. *Biochemistry* **1995**, *34*, 6795.
- (6) Frank, H. S.; Franks, F. J. *Chem. Phys.* **1968**, *48*, 4746.
- (7) Collins, K. D.; Washabaugh, M. W. *Q. Rev. Biophys.* **1985**, *18*, 323.
- (8) (a) Schelman, J. A. *Comput. Rend. Trav. Lab. Carlsberg, Ser. Chim.* **1955**, *29*, 223. (b) Kreschek, G. C.; H. A. Scheraga, *J. Phys. Chem.* **1965**, *69*, 1704. (c) Stokes, R. H. *Aust. K. Chem.* **1967**, *20*, 2087.
- (9) Åstrand, P.-O.; Wallqvist, A.; Karlström, G.; Linse, P. *J. Chem. Phys.* **1991**, *95*, 8419.
- (10) Kallies, B. *Phys. Chem. Chem. Phys.* **2002**, *4*, 86.
- (11) Soper, A. K.; Castner, E. W.; Luzar, A. *Biophys. Chem.* **2003**, *105*, 649.
- (12) Tanaka, H.; Nakanishi, K.; Touhara, H. *J. Chem. Phys.* **1985**, *82*, 5184.
- (13) Hernández-Cobos, J.; Ortega-Blake, I.; Bonilla-Marín, M.; Moreno-Bello, M. *J. Chem. Phys.* **1993**, *99*, 9122.
- (14) Grdadolnik, J. *J. Mol. Struct.* **2002**, *615*, 177.
- (15) Kokot, S.; Czarnik-Matusewicz, B.; Ozaki, Y. *Biospectrosc.* **2002**, *67*, 456.
- (16) Jung, Y. M.; Shin, H. S.; Czarnik-Matusewicz, B.; Noda, I.; Kim, S. B. *Appl. Spectrosc.* **2002**, *12*, 1568.
- (17) Czarnecki, M. A.; Czarnik-Matusewicz, B.; Ozaki, Y.; Iwahashi, M. *J. Phys. Chem. A* **2000**, *104*, 4906.
- (18) Venyaminov, S. Y.; Prendergast, F. G. *Anal. Biochem.* **1997**, *248*, 234.
- (19) Barclay, V. J.; Bonner, R. F.; Hamilton I. P. *Anal. Chem.* **1997**, *69*, 78.
- (20) Berry, R. J.; Ozaki, Y. *Appl. Spectrosc.* **2002**, *56*, 1462.
- (21) Czarnecki, M. A. *Appl. Spectrosc.* **2003**, *57*, 107.
- (22) Noda, I.; Ozaki, Y. *Appl. Spectrosc.* **2003**, *57*, 110.
- (23) Yu, Z. W.; Noda, I. *Appl. Spectrosc.* **2003**, *57*, 164.
- (24) Rousseau, B.; Van Alsenoy, C.; Keuleers, R.; Desseyn, H. O. *J. Phys. Chem. A* **1998**, *102*, 6540.
- (25) Hoccart, X.; Turrell, G. *J. Chem. Phys.* **1993**, *99*, 8498.
- (26) Lee, C.; Stahlberg, E. A.; Fitzgerald, G. *J. Phys. Chem.* **1995**, *99*, 17737.
- (27) Liao, H.-L.; Chu, S.-Y. *New J. Chem.* **2003**, *27*, 421.
- (28) Masunov, A.; Dannenberg, J. J. *J. Phys. Chem. A* **1999**, *103*, 178.
- (29) Gilli, P.; Bertolasi, V.; Ferretti, V.; Gilli, G. *J. Am. Chem. Soc.* **1994**, *116*, 909.
- (30) Sokolić, F.; Idrissi, A.; Perera, A. *J. Mol. Liq.* **2002**, *101*, 81.
- (31) Weerasinghe, S.; Smith, P. E. *J. Chem. Phys.* **2003**, *118*, 5901.
- (32) Masunov A.; Dannenberg, J. J. *J. Phys. Chem. B* **2000**, *104*, 806.
- (33) Swaminathan, S.; Craven, B. M.; McMullan, R. K. *Acta Crystallogr. B* **1984**, *40*, 300.
- (34) Rousseau, B.; Keuleers, R.; Desseyn, H. O.; Geise, H. J.; Van Alsenoy, C. *Chem. Phys. Lett.* **1999**, *302*, 55.
- (35) Murayama, K.; Czarnik-Matusewicz, B.; Wu, Y.; Tsenkova, R.; Ozaki, Y. *Appl. Spectrosc.* **2000**, *54*, 978.